CHAPTER 4

A perspective on designing chiral organic magnetic molecules with unusual behavior in magnetic exchange coupling

Abstract

In the fourth chapter we have designed a total of nine diradical based organic chiral magnetic molecules with allene and cumulene couplers and subsequently the magnetic property has been studied by DFT. It is found that with an increase in length of the coupler, a remarkable increase in spin density within the coupler takes place. An increase in the length of the coupler reduces the energy of LUMO, and a smaller HOMO-LUMO gap facilitates stronger magnetic coupling and thereby a higher magnetic exchange coupling constant (*J*). This observation is supported by the occupation number of natural orbitals.

4.1 Introduction

Chirality is of utmost importance as it plays a key role not only in the life forms but also in pharmaceutical, agricultural and other chemical industries.[1] At present, chiral organic molecules are of extensive interest to organic chemists as well as pharmaceutical chemists.[2] Galán-Mascarós et al. have synthesized molecular materials with ferromagnetism, metal-like conductivity and chirality.[3] When chirality appears in the structure of atoms in a solid having unpaired electrons, the chiral lattice favor a screw like arrangement of the magnetic moments of unpaired electrons, but they must compete with ferromagnetic exchange, that attempts to align all the magnetic moments in the same direction. These chiral lattice are known as chiral magnets.[4] On the other hand, chiral magnetic molecules with ferromagnetic interaction can also be regarded as chiral magnet.[5] Stable chiral magnets are important ingredients for future data storage, spintronic device[6] and other applications for their fascinating properties.[4] The most important phenomena shown by chiral magnets are the magneto-chiral effect which occurs in chiral media in presence of a magnetic field.[7] The synthesized chiral magnets are mainly inorganic or metallo-organic in nature.[8,9] It is observed that chiral magnets, particularly manganese silicide (MnSi), a cubic intermetallic compound that has no inversion symmetry i.e, with a noncentrosymmetric crystal structure,[10] have attracted interest over the last few years and they may one day reach a degree of functionality similar to that of chiral liquid crystals.[4] But in last few decades, the search for new ferromagnetic materials based on organic diradicals has generated tremendous interest.[11-13] Organic radicals[11] have been widely studied for their versatile applicability in the field of magnetism,[14] and for their superconductivity,[15] spintronic properties,[16] photomagnetic behaviour[17] and so on. In case of organic diradicals, the magnetic interaction between two radical centers normally depends on the couplers which connect the radical centers.[18] A series of nitronylnitroxide (NN) diradicals with linear conjugated couplers have been studied by Ali and Datta, and they reported that the magnetic exchange coupling constant value decreases gradually with increasing conjugation length of the coupler.[19] It has been found that chains containing sp-hybridized carbon atoms are fascinating due to their unique linear structure and interesting physical properties.[20] Allenes (1, 2-propadiene derivatives) are an important class of compounds and have gained increasing attraction as interesting building blocks in synthetic organic chemistry.[21] Cumulenes with odd number of carbon atoms have π-systems that are spatially orthogonal with each other and therefore these systems contain a chiral axis and their two pairs of substituent are in two perpendicular planes, giving rise to enantiomers.[22] Skibar et al. have synthesized cumulenes containing 7 carbon atoms.[23] Januszewski et al. also have synthesized and predicted the properties of long cumulenes containing up to 10 carbon atoms.[24] Cumulenes find major application in molecular machines (nano-mechanics), molecular wires (nano-electronics), nonlinear optics, and molecular sensors due to their unique electronic structures.[25] It is found that among all conjugated oligomers, cumulene wires with odd number of carbon atoms show the highest conductance with metallic-like ballistic transport behavior.[26]

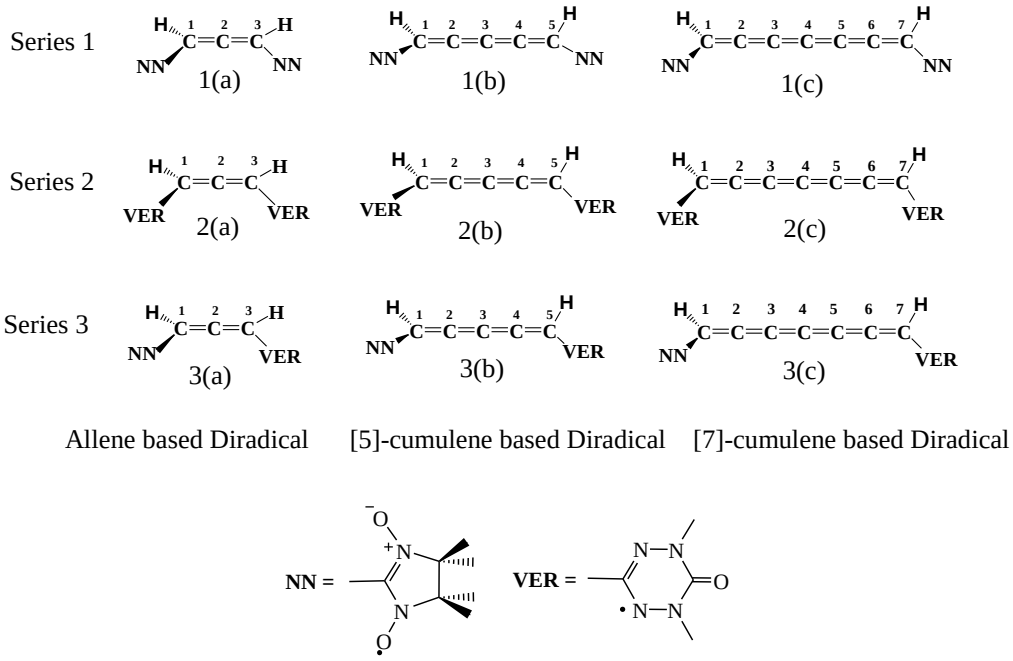

Figure 4.1 Allene- and cumulene-based diradicals. [5] and [7] indicates the number of carbon atoms in a coupler.

We have designed allene and cumulene (containing odd number of carbon atoms) based diradical systems that are shown in Figure 4.1 and have studied the magnetic property of these diradicals in detailed as an estimation of the intramolecular exchange coupling constant is necessary before synthesizing a successful magnetic material based on organic diradicals or transition metal complexes. These designed molecules may be used as molecular building block for organic chiral magnetic solids.

4.2 Theoretical Background

The magnetic exchange interaction between two magnetic sites 1 and 2 is generally express by the Heisenberg spin Hamiltonian $\hat{H} = -2J\hat{S}_1 \bullet \hat{S}_2$, where $\hat{S}_1$ and $\hat{S}_2$ are the respective spin angular momentum operators and J is the exchange coupling constant between two magnetic centers. When J is positive, the high-spin state is lower in energy, and the coupling is said to be ferromagnetic. A negative value of J is representative of antiferromagnetic interaction in the diradical and a low-spin state is the ground state. For a diradical containing a single unpaired electron on each site, J can be represented as $E_{(S=1)} - E_{(S=0)} = -2J$.

Multiconfiguration approaches are suitable to describe pure spin states in an appropriate manner; but these methods are resource intensive and not used in this work. To circumvent this issue, broken symmetry (BS) approach by Noodleman et

al.[27-30] in DFT framework is a more useful alternative to evaluate *J* that can eventually lead to an estimate of the energy of diradical singlet. The ideal BS state is a weighted average of the singlet and the triplet, and has an M_S equal to zero. The ideal triplet (T) state has an $\langle S^2 \rangle$ = 2, whereas $\langle S^2 \rangle$ = 1 in the ideal BS state and that results E(BS) $-E$(T) =J. However in actual calculation approximate $\langle S^2 \rangle$ values are obtained, and hence BS solution is often found to be spin contaminated. Therefore, a correction is needed to calculate the coupling constant.

The spin projected formula given by Yamaguchi[31-34] for the evaluation of magnetic exchange coupling constant (*J*) is free from such spin contamination and applicable for both low and high overlap between magnetic orbitals, which can be written as $J = (E_{BS} - E_{HS}) \Big/ \left(\left\langle S^2 \right\rangle_{HS} - \left\langle S^2 \right\rangle_{BS} \right)$ where E_{BS}, E_{HS}, $\langle S^2 \rangle_{BS}$, and $\langle S^2 \rangle_{HS}$ are the energies and average spin square values for the BS and high-spin states, respectively.

4.3 Computational Strategy

The molecular structure of all the diradicals have been fully optimized in each spin state by hybrid exchange-correlation functionals B3LYP and M06 in combination with 6-311++G(d,p) basis set within the unrestricted formalism using Gaussian09 quantum chemical package.[35] A broken symmetry (BS) singlet solution has been performed for mixing of the HOMO and the LUMO. To obtain open shell BS singlet solution "guess=mix" keyword is used. The magnetic exchange coupling constant (*J*) value for each molecule has been estimated from the energies of triplet and BS states at the same level of theory using the spin projected formula given by Yamaguchi.[31-34] To confirm the enantiomeric nature of our designed systems, we analyze the vibrational circular dichroism (VCD) spectra using freq= vcd keyword. Detailed analyses of geometrical parameters, the spin density distribution, molecular orbital as well as natural orbital occupancies have been calculated with the optimized geometry.

4.4 Results and Discussion

It is well-known that the two enantiomers of a chiral compound show optical rotation value of same angle but in opposite direction in presence of plane-polarized light. The absolute configuration of a chiral molecule can be determined from its vibrational circular dichroism (VCD) spectrum as the VCD spectra of the two enantiomers of a chiral molecule are equal in magnitude and opposite in sign.[2] Here we have tried to verify the enantiomeric relationship between our designed chiral molecules. For series 2 diradicals (in Figure 4.2), calculated VCD spectra (in Figure 4.3) confirm the stereochemistry as well as the enantiomeric relationship between them.

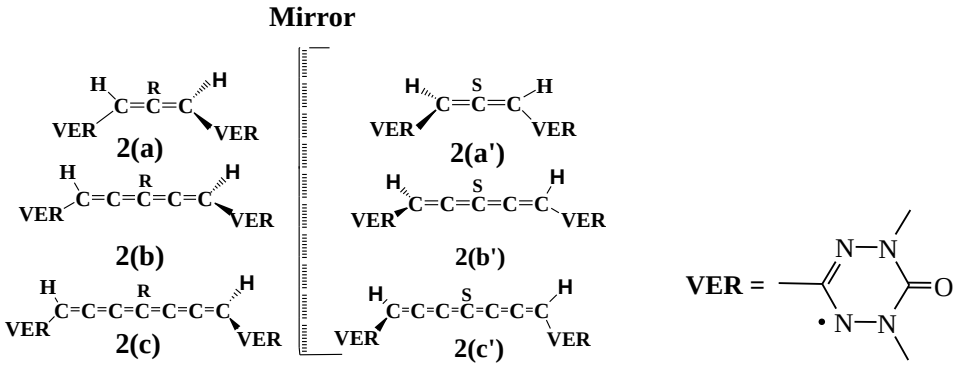

Figure 4.2 *R* and *S* configuration of the designed diradicals of series 2.

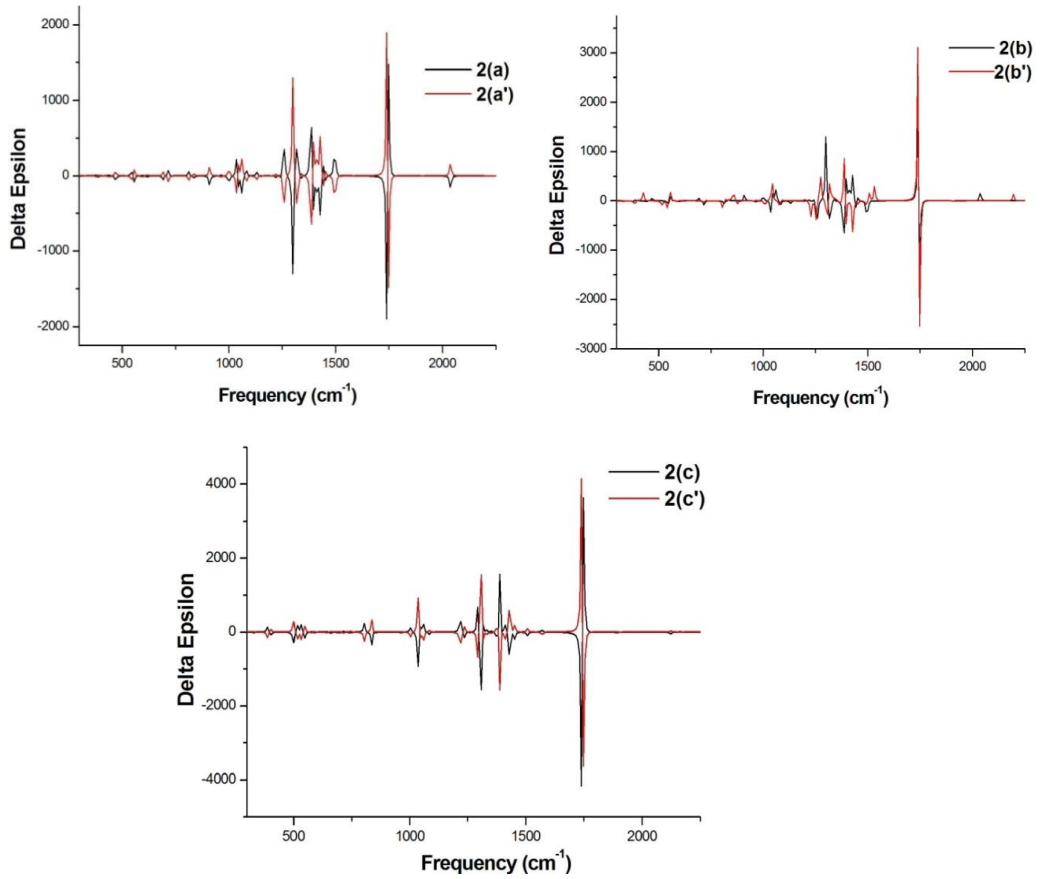

Figure 4.3 VCD spectra of two enantiomers of series 2 (We have calculated the VCD spectra of the diradicals using B3LYP functional and 6-311++G(d,p) basis set on the top of optimized geometry of M06 functional with 6-311++G(d,p) basis set).

The other diradicals (series 1 and series 3) have similar couplers; therefore it is obvious that they will follow the same trend as series 2. The point here is that the form of the Hamiltonian guarantees the magnetic exchange coupling constant of the diradical based chiral enantiomers to be equal in magnitude.

4.4.1 Magnetic exchange coupling constant

The calculated magnetic exchange coupling constants of all the diradicals are listed in Table 4.1. The consistency of magnetic exchange coupling constant values have been confirmed using two different exchange-correlation functionals (B3LYP and M06). It is observed that although the values of coupling constants are different for different methods, they follow the similar trend. From Table 4.1 it is observed that with the increase in chain length of the coupler from the allene based diradical to the [5]-cumulene based diradical, the magnetic exchange coupling constant increases almost 2-fold, and again upon the transition from the [5]-cumulene based diradical to the [7]-cumulene based diradical, the coupling constant further increases approximately by 2-fold, which contradicts the fact that the level of magnetic exchange decreases with an increase in the length of conjugated systems.[19] Therefore, it can be argued that there must be a major contribution of the coupler in magnetic exchange pathway and this observation demands a detailed investigation of electronic structure of these couplers. If we compare the coupling constant of same coupler with different radicals, we can see that the NN based diradicals have highest coupling constant and VER based diradicals have lowest one, combination of two radicals NN and VER gives the coupling constant in between. Thus, we can conclude that the nitronyl nitroxide radical is more suitable for obtaining a coupling constant higher than that of verdazyl radical with allene and cumulene couplers.

Table 4.1 The energy (a.u.),$\langle S^2 \rangle$ and magnetic exchange coupling constant (J in cm^{-1}) of designed diradicals (from series 1 to series 3).

		B3LYP/6-311++G(d,p)			M06/6-311++G(d,p)			
Systems		**Triplet**	**BS**	***J***		**Triplet**	**BS**	***J***
1(a)	E	-1183.41922	-1183.41900	47.66	E	-1182.62355	-1182.62326	63.17
	$\langle S^2 \rangle$	2.136	1.123		$\langle S^2 \rangle$	2.134	1.116	
1(b)	E	-1259.59164	-1259.59117	99.09	E	-1258.73505	-1258.73440	146.28
	$\langle S^2 \rangle$	2.207	1.166		$\langle S^2 \rangle$	2.134	1.158	
1(c)	E	-1335.76802	-1335.76716	171.28	E	-1334.85150	-1334.85020	244.31
	$\langle S^2 \rangle$	2.319	1.217		$\langle S^2 \rangle$	2.384	1.215	
2(a)	E	-1016.17752	-1016.17745	15.30	E	-1015.50571	-1015.50560	22.96
	$\langle S^2 \rangle$	2.050	1.046		$\langle S^2 \rangle$	2.050	1.044	
2(b)	E	-1092.34903	-1092.34889	30.36	E	-1091.61679	-1091.61658	45.00
	$\langle S^2 \rangle$	2.068	1.056		$\langle S^2 \rangle$	2.073	1.054	
2(c)	E	-1168.52398	-1168.52373	53.17	E	-1167.73165	-1167.73123	86.95
	$\langle S^2 \rangle$	2.100	1.068		$\langle S^2 \rangle$	2.132	1.068	
3(a)	E	-1099.79801	-1099.79788	28.33	E	-1099.06411	-1099.06393	39.14
	$\langle S^2 \rangle$	2.092	1.085		$\langle S^2 \rangle$	2.090	1.080	
3(b)	E	-1175.97033	-1175.97007	55.84	E	-1175.17589	-1175.17552	78.62
	$\langle S^2 \rangle$	2.136	1.114		$\langle S^2 \rangle$	2.143	1.109	
3(c)	E	-1252.14603	-1252.14557	95.42	E	-1251.29167	-1251.29093	147.65
	$\langle S^2 \rangle$	2.209	1.151		$\langle S^2 \rangle$	2.258	1.156	

We have calculated the absolute energy values of the diradicals as $\frac{1}{2}[E_{NN}^{T} + E_{VER}^{T}]$ and for mixed radical systems given in Table 4.2 and found that for allene based diradicals the energy difference is as small as 0.00036 a.u. and for longer cumulene there is no energy difference at all, which suggests that the interaction between radicals at the two ends of the molecules is not radical specific and decreases with an increase in the length of the carbon chain.

Table 4.2 Absolute energies of the diradicals as $\frac{1}{2}[E_{NN}^{T} + E_{VER}^{T}]$ and for mixed radical systems in their triplet state (E_{NN}^{T} represents the energy of series 1 diradicals, E_{VER}^{T} represents the energy of series 2 diradicals, and E_{Mixed} represents the energy of series 3 diradicals).

Systems	E_{NN}^{T} **(a.u.)**	E_{VER}^{T}**(a.u.)**	$\overline{E}_{\text{pure}} = \frac{1}{2}[E_{NN}^{T} + E_{VER}^{T}]$**(a.u.)**	E_{Mixed} **(a.u.)**	$\Delta E = (\overline{E}_{\text{Pure}} - E_{\text{Mixed}})$ **(a.u.)**
Allene based Diradical	-1183.41922	-1016.17752	-1099.79837	-1099.79801	-0.00036
[5]-cumulene based Diradical	-1259.59164	-1092.34903	-1175.97034	-1175.97033	0.00001
[7]-cumulene based Diradical	-1335.76802	-1168.52398	-1252.14600	-1252.14603	0.00003

4.4.2 Spin density distribution

The spin density of DFT based approach can give us an insight about the spin polarization mechanism for magnetic exchange coupling within the molecule. Exchange coupling constant between two magnetic sites largely depends on the delocalization of π-electron densities between them. Hence, to understand the anomalous increase in magnitude of *J*, we have done the spin density distribution analysis. Hund's rule based spin density alternation rule[36,37] helps to predict the nature of magnetic interaction for diradicals with different couplers. Ferromagnetic exchange coupling takes place between two spin centers when they are connected by even number of conjugated bonds and antiferromagnetism occurs for odd number of bonds.[36,37] Spin density distribution of the diradicals in their high-spin states (Figure 4.4) confirm that all these diradicals have intramolecular ferromagnetic coupling.

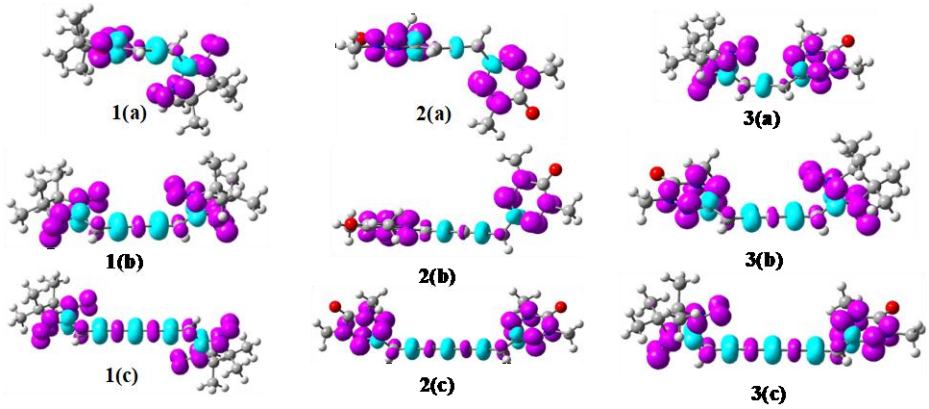

Figure 4.4 Spin density plot of all the designed diradicals in their triplet states (B3LYP/6-311++G(d,p)), (iso value 0.004), magenta and sky colors represent the α and β spins respectively.

The spin density on different atoms of coupler and also the total spin density of coupler in designed diradicals are reported in Table 4.3. Hermann et al. have proposed that cumulene based systems with even number of carbon centers, the spin delocalization onto the chain increases as the length of the chain gets longer.[38] For our designed systems it is also found that with increase in chain length of the coupler, spin density on different atoms of coupler as well as the total spin density on coupler increases, which is quite contradictory from the concept that with increase in chain length of conjugated systems the spin density on the coupler reduces.[19] Hence as argued in the previous subsection, there must be some special reason which facilitates the spin polarization in such systems.

Table 4.3 Spin density distribution on each atom of coupler and total spin density of coupler in designed diradicals in their triplet state (B3LYP/6-311++G(d,p)).

Systems	**Spin density on different atoms of coupler**							**Total spin density**
	C_1	C_2	C_3	C_4	C_5	C_6	C_7	
1(a)	0.0768	-0.2655	0.0768	--------	--------	--------	--------	-0.1120
1(b)	0.1072	-0.2664	0.1572	-0.2665	0.1071	--------	--------	-0.1614
1(c)	0.1501	-0.3004	0.2041	-0.3196	0.2041	-0.3004	0.1501	-0.2120
2(a)	0.0616	-0.141	0.0616	-------	--------	--------	--------	-0.0177
2(b)	0.0831	-0.1341	0.0652	-0.1341	0.0831	--------	--------	-0.0366
2(c)	0.1223	-0.1659	0.0899	-0.1396	0.0899	-0.1659	0.1223	-0.0470
3(a)	0.0638	-0.1862	0.0683	---------	--------	--------	--------	-0.0541
3(b)	0.1025	-0.2095	0.114	-0.1969	0.0953	--------	-------	-0.0946
3(c)	0.1437	-0.2437	0.1711	-0.2488	0.1469	-0.2316	0.1362	-0.1262

4.4.3 Spin polarization

Chiral allene and cumulene couplers contain even number of π-bonds in perpendicular planes; therefore the two end π-bonds are perpendicular to each other. A close inspection of the spin density plot in Figure 4.5 for series 1 diradicals point to the fact that the spin density distribution of π-electrons of two end carbon atoms of the coupler are individually directed along two Cartesian axes (y and z direction). But for rest of the carbon atoms within the coupler, spin polarization of π-electrons is along both the y and z directions collectively, causing a large accumulation of spin density for the middle carbons of the coupler chain. Plausible mechanistic pathway of spin polarization within the coupler is shown in Figure 4.6.

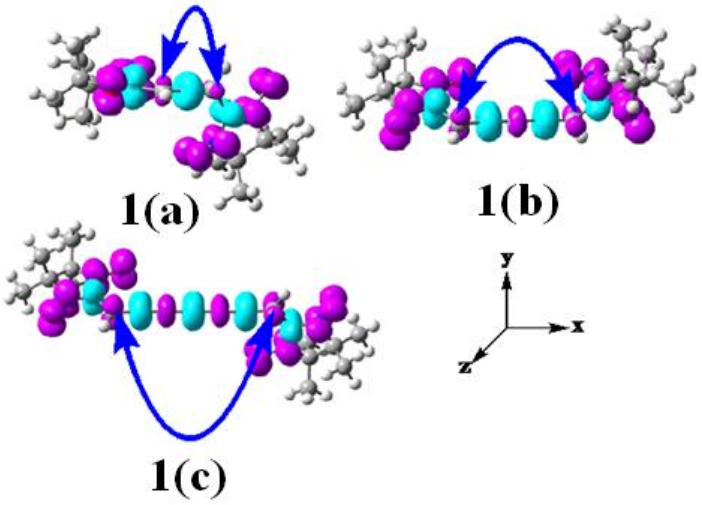

Figure 4.5 Spin density plot for the diradicals of series 1 in their triplet states (B3LYP/6-311++G(d,p)) (iso value 0.004), magenta and sky colors represent the α and β spins respectively. Blue arrow represents two end carbons of coupler.

To explain the increase in spin density upon addition of carbon center within the coupler, and simultaneously to explain the contradictory behavior of spin polarization in cumulenes with that of conjugated systems (*i.e.*, alternating σ and π bonds), detailed investigation of mechanistic pathway of spin polarization was conducted. Figure 4.6 shows that the two end carbons in allene based diradical contain one π-bonding electron on each of them, but the central carbon contains two π-bonding electrons in two different *p* orbitals at a time. Therefore, for allene based diradicals, spin polarization is greater in middle carbon compared to the end carbons. Now while comparing the allene based diradical with [5]-cumulene based diradical, one finds that former contains only one carbon with two π-electrons at central region of the coupler but later contains three carbons with two π-electrons on each. As a result [5]-cumulene based diradical has higher accumulation of spin density on each carbon of coupler compared to allene based diradical. A similar trend in [7]-cumulene based diradical is also observed. Thus, one can surmise that spin polarization

increases considerably with increase in the number of carbon centers of coupler in cumulene systems.

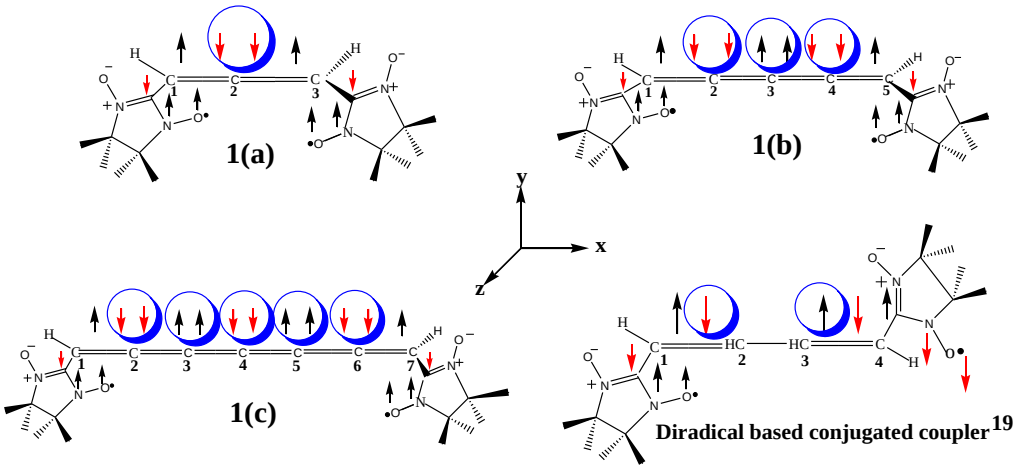

Figure 4.6 Spin polarization of π electron within the coupler (for series 1).

Upon comparison of the spin density of cumulene with that of the conjugated coupler, it is found that for conjugated coupler based diradicals, each carbon atom of the coupler contains one π-electron on each and no such enhancement of spin polarization occurs; moreover, a decrease in spin density with an increase in the chain length of the coupler is observed as the distance between the radical centers increases. Figure 4.7 is a plot of the coupling constant versus the distance between the radical centers that clearly shows the variation of the coupling constant with distance.

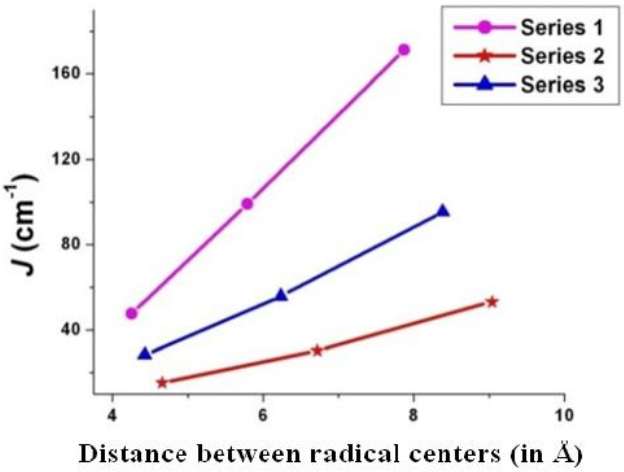

Figure 4.7 Plot of magnetic exchange coupling constant vs. distance (in Å) between radical centers (B3LYP/6-311++G(d,p)).

Therefore a high level of accumulation of spin density within the coupler overcomes the distance factor between the radical centers in case of cumulene based diradicals and higher magnetic exchange coupling results with the increase in the length of the coupler.

4.4.4 Molecular structures

A small change in molecular structure can lead to a drastic change in the magnetic coupling constant.[39] Therefore, it is important to study the molecular structure of the allene and cumulene based diradicals in order to understand their magnetic behavior. The optimized geometrical parameters of our designed diradicals are reported in Table 4.4 and Table 4.5.

Table 4.4 Bond distance between two atoms and the average bond distance of the couplers for the designed diradicals in their triplet state (B3LYP/6-311++G(d,p)). All bonds are in pm unit. (L is the connecting atom of left radical center and R is the connecting atom of right radical center respectively).

System	Bond distance						Average bond distance	Distance between C_1-L	Distance between C_3-R	Distance Between C_5-R	Distance between C_7-R
	C_1=C_2	C_2=C_3	C_3=C_4	C4=C_5	C_5=C_6	C_6=C_7					
1(a)	131.1	131.1	-------	-------	-------	-------	131.1	143.8	143.8	--------	--------
1(b)	132.6	127.0	127.0	132.6	-------	-------	129.8	142.8	--------	142.8	--------
1(c)	133.3	126.4	128.1	128.1	126.4	133.3	129.3	142.3	--------	--------	142.3
2(a)	130.7	130.7	-------	-------	-------	-------	130.7	147.3	147.3	--------	--------
2(b)	131.9	127.2	127.2	131.9	-------	-------	129.5	146.6	--------	146.6	--------
2(c)	132.3	126.7	128.0	128.0	126.7	132.3	129.0	146.2	--------	--------	146.2
3(a)	131.3	130.5	-------	-------	-------	-------	130.1	144.0	147.2	--------	--------
3(b)	132.6	126.9	127.3	131.8	-------	-------	129.7	142.9	--------	146.5	--------
3(c)	133.3	126.3	128.3	127.9	126.8	132.4	129.2	142.3	--------	--------	146.2

The most important structural aspect is the bond distance alteration of the cumulene moiety. Our calculations predict a distinct alternation of adjacent C=C bonds, the first and last bond lengths for all the diradicals are approximately close to the double bond length in ethylene (132pm). The central double bond distance in [5]-cumulene based diradicals are approximately 127pm and their values are in between the double bond length in ethylene (132pm) and the C≡C triple bond length in acetylene (121.2 pm).The central bond distance for [7]-cumulene are also approximately 128 pm and double bond lengths elsewhere in the bridge chain equal 126 pm and their values are in between the double bond length in ethylene (132pm) and the C≡C triple bond length in acetylene (121.2 pm). When two different groups are included, all the

double bond lengths become unequal (see series3). These different bond lengths are indicative of electronically different bonding situations.

Another important point is that the average C-C bond length tends to decrease with increase in cumulene chain length in a particular series, as for series 1 the values are 131.1pm, 129.8pm, and 129.3 pm for 1 (a), 1(b) and 1(c) respectively and this is closer to a C=C double bond distance, as expected. It is observed that with decrease in the average bond length in each series, there is a possibility of increase in s-character of the coupler. The higher the s-character the greater is the electronegativity of that atom, and higher is the possibility to localize the spin density on that atom, which facilitates the higher spin densities on the coupler with increase in length. From Table 4.4 it is also clear that with increase in length of the coupler the distance between carbon atoms of the coupler and the radical centers decreases in each series, therefore the conjugation between the coupler and the radical center increases. Thus, ultimately a better π-interaction results with the increase in the chain length of the coupler.

The computed bond angle between the carbon atoms in the coupler are described in Table 4.5. It is confirmed that the bond angle of the coupler deviates from the exact angle of allene (180º), hence they are the systems with a nonlinear C=C=C framework, and are characterized by slightly deviated orthogonal π-bonds. This bending is higher in case of allene based diradicals compared to cumulene based diradicals. For this the allene π-system is significantly disturbed, and the central carbon atom is no longer sp-hybridized as in typical all-carbon allenes. Now, comparing diradical substituted allene with their higher homologue it is found that with increase in the chain length the middle allene counterpart goes nearly 180º (e.g, for 1(a) $\angle c_1\text{-}c_2\text{-}c_3$=173.87º, for 1(b) $\angle c_2\text{-}c_3\text{-}c_4$=177.97º, and for 1(c) $\angle c_3\text{-}c_4\text{-}c_5$=179.8º). Hence, there is relatively strong π-interaction with increasing chain length in each series and the coupling constant increases accordingly.

Table 4.5 Bond angle for the couplers in the diradicals in series 1-3 in their triplet state (B3LYP/6-311++G(d,p)).

Systems	**Bond angle/ º**				
	$\angle c_1\text{-}c_2\text{-}c_3$	$\angle c_2\text{-}c_3\text{-}c_4$	$\angle c_3\text{-}c_4\text{-}c_5$	$\angle c_4\text{-}c_5\text{-}c_6$	$\angle c_5\text{-}c_6\text{-}c_7$
1(a)	173.87	---------	---------	----------	---------
1(b)	174.35	177.97	174.35	--------	---------
1(c)	174.33	178.42	179.8	178.41	174.33
2(a)	177.92	----------	----------	---------	----------
2(b)	178.12	179.76	178.11	---------	----------
2(c)	178.13	179.88	179.95	179.87	178.14
3(a)	175.75	---------	----------	----------	----------
3(b)	174.54	178.49	178.23	---------	----------
3(c)	174.44	178.59	179.76	179.83	178.11

4.4.5 Molecular orbital analysis

The shape of molecular orbitals play a major role in determining the magnetic properties of the diradicals, electronic transport etc.[40] Frontier molecular orbitals (FMOs) of all the axially chiral allene and cumulene based diradical are presented in Figure 4.8. According to Borden and co-workers when the nonbonding molecular orbitals of a diradical have no atoms in common i.e., disjoint in nature, the diradicals favor antiferromagnetic state as ground state. The non-disjoint SOMOs favor ferromagnetic ground state. From Figure 4.8 one can see that α-SOMOs of diradicals in series 1 and 2 are non-disjoint and α-SOMOs of diradicals in series 3 are disjoint although all the diradicals are ferromagnetic in nature.

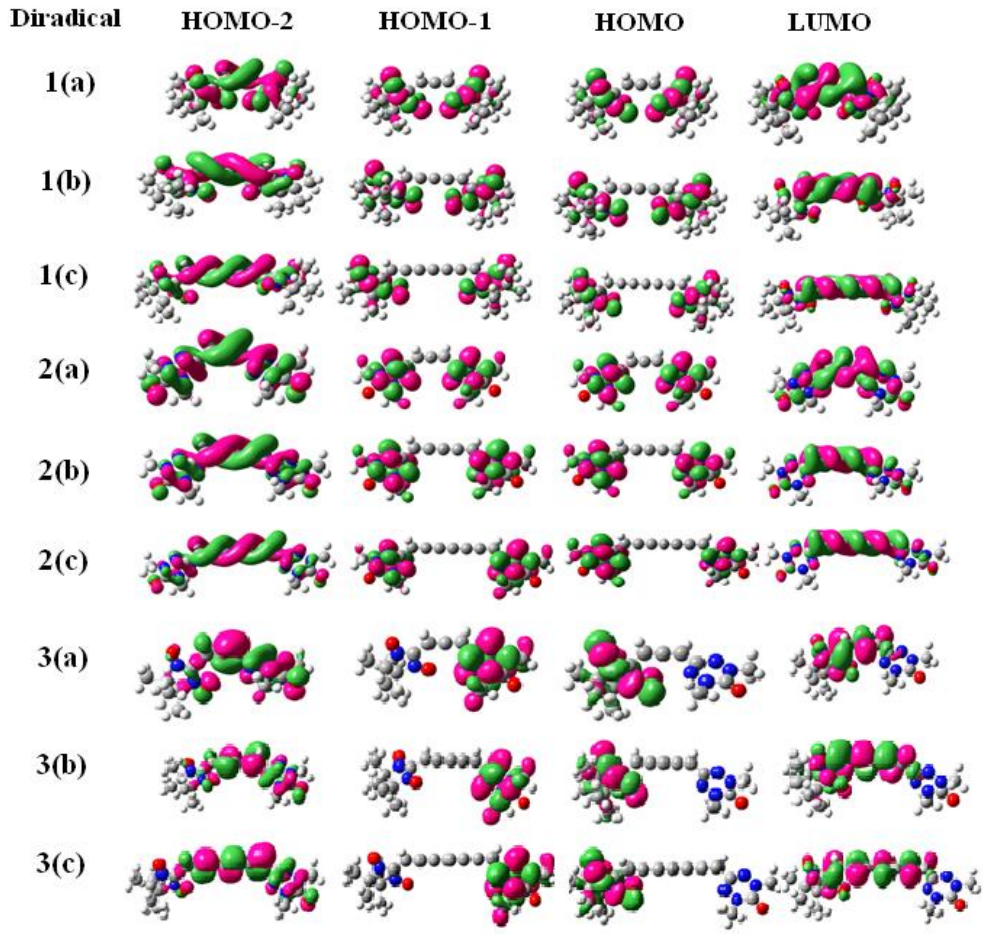

Figure 4.8 Spatial distribution of molecular orbitals of all the diradicals in their triplet states (B3LYP/6-311++G(d,p)) (iso value 0.02), green and pink colors represent the different phase of the orbital coefficients.

We have carried out molecular orbital analysis of diradical 1 and 2 with varying geometry given in Figure 4.9, to check the stability of non-disjoint nature of the SOMOs and found that the SOMOs are unaltered upon structural changes. Thus Borden's analogy [41,42] which is derived for alternant hydrocarbons does not fit for the disjoint diradicals in series 3. Thus, it may be surmised that Borden's analogy which is derived for alternant hydrocarbons does not fit for these diradicals and such systems follow a different mechanism for magnetic interaction.

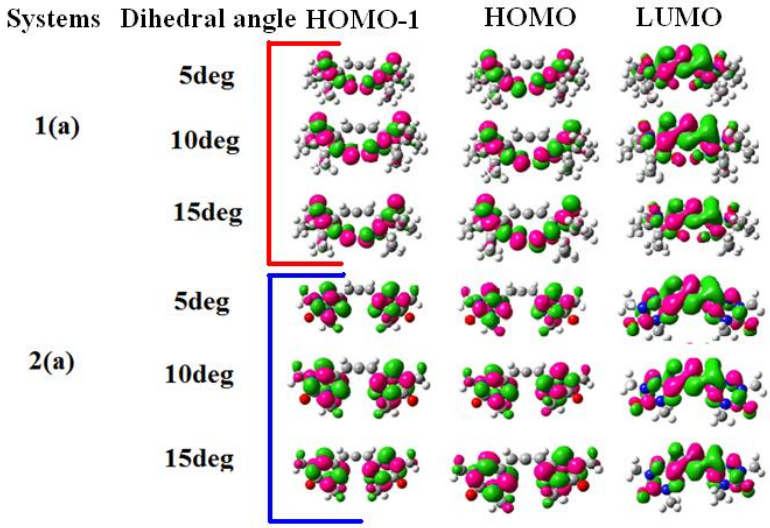

Figure 4.9 Spatial distribution of molecular orbitals of the diradicals with varying geometry in their triplet states (B3LYP/6-311++G(d,p)) (iso value 0.02), green and pink colors represent the different phase of the orbital coefficients.

The molecular orbital analysis of the BS determinant of diradical based allene in Figure 4.10 shows that for 1(a) and 2(a) diradicals, the α-HOMO and β-HOMO are on the two individual radical centers. However α-SOMOs of the triplet state for those diradicals are distributed collectively on two radical centers. But for series 3 diradicals (3(a)) the shape of α-HOMO and β-HOMO of BS determinant and α-SOMOs of triplet state are same. Therefore, the SOMOs of BS determinant and triplet state are not exactly same for all the diradicals but are distributed only over radical centers.

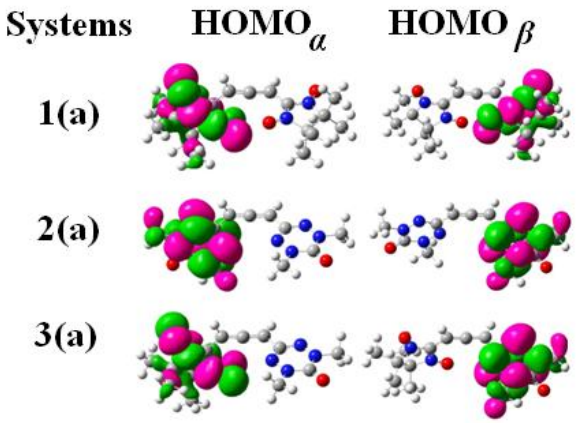

Figure 4.10 The molecular orbital of the diradicals (HOMO$_\alpha$ and HOMO$_\beta$) in their Broken symmetry state (B3LYP/6-311++G(d,p)) (iso value 0.02), green and pink colors represent the different phase of the orbital coefficients.

4.4.6 Mechanism of magnetic interaction

Molecular orbital takes an important role to understand the magnetic coupling between two radical centers. It is known that the SOMOs are mainly responsible for magnetic interaction in diradicals through itinerant exchange[41-44] and the low SOMO–SOMO gap or degenerate SOMOs produces strong magnetic exchange coupling constant. The SOMO–SOMO energy gap, HOMO–LUMO energy gap for the designed diradicals are listed in Table 4.6. We observe from the Table 4.6 that for series 1 and 2, the two SOMOs are almost degenerate although they have different values of *J* in each series. Another interesting point is that for diradicals 3(a) and 3(b) SOMO–SOMO gap is highest and equal in magnitude but shows the different *J* values. So, the SOMO–SOMO gap is not the only guiding factor to determine the extent of magnetic interaction, there must be some other factor which guides magnetic exchange. In couple of our recent works, we have studied that the SOMO–SOMO gap is not responsible for the strength of magnetic coupling, rather HOMO–LUMO gap plays a more important role.[39,45,46] If we focus on the energy difference between HOMO and LUMO in this study, it has been found that on going from diradical based allene to its higher homologue ([5]- and [7]-cumulene) in each series, there is a smooth decrease in HOMO–LUMO energy gap. Hermann et al. also have showed that the α-HOMO–α-LUMO gaps decreases with increasing carbon chain lengths of cumulene based systems containing even number of carbon centers.[38] Therefore, it can be concluded that diradicals with low HOMO–LUMO gap facilitates the strong magnetic coupling constant and the diradicals based on allene and cumulene couplers with low HOMO–LUMO gap will be the promising candidate to design chiral organic magnetic molecules.

Table 4.6 Energy (in eV) of HOMO–2, HOMO–1, HOMO and LUMO for all the diradicals and the energy difference (in eV) between SOMO1 $(HOMO)_{\alpha}$–SOMO2 $(HOMO–1)_{\alpha}$ (ΔE_{SS}) and $HOMO_{\alpha}$–$LUMO_{\alpha}$ (ΔE_{HL}) and magnetic exchange coupling constant (J in cm^{-1}) in their triplet state (B3LYP/6-311++G(d,p)).

System	E_{HOMO-2}	E_{HOMO-1}	E_{HOMO}	E_{LUMO}	ΔE_{SS}	ΔE_{HL}	J
1(a)	-6.89275	-5.29989	-5.29309	-1.58143	0.01	3.71	47.66
1(b)	-6.54971	-5.39002	-5.38653	-2.36083	0.00	3.03	99.09
1(c)	-6.29637	-5.47614	-5.47329	-2.83002	0.00	2.64	171.28
2(a)	-7.06015	-5.59234	-5.57656	-1.44088	0.02	4.14	15.30
2(b)	-6.65889	-5.63969	-5.63901	-2.28864	0.00	3.35	30.36
2(c)	-6.39022	-5.68584	-5.68584	-2.83331	0.00	2.85	53.17
3(a)	-6.89035	-5.49982	-5.36784	-1.64687	0.13	3.72	28.33
3(b)	-6.53529	-5.57941	-5.44784	-2.44366	0.13	3.00	55.84
3(c)	-6.29033	-5.61574	-5.52594	-2.73263	0.09	2.79	95.42

Our designed diradicals based on allene, [5]- and [7]-cumulene coupler (containing odd number of carbon atoms) has two π-conjugations that are mutually perpendicular to each other. Imamura and Aoki have proposed that polyyne has two π-conjugated systems mutually perpendicular to each other and both the π-conjugations have a tendency to follow a bond alternation that originates a competition in between them.[47-49] With increase in the length of the polyyne chain, a remarkable transition in the molecular structure takes place from almost equidistant bond structure to an intensely alternating bond structure, that causes a lifting of the HOMO level and a lowering of LUMO level. As a result there is a sudden decrease in HOMO–LUMO gap with increase in the length of the polyyne chains. The orbital phases of two mutually perpendicular π-conjugations for our designed diradicals are shown in Figure 4.11.

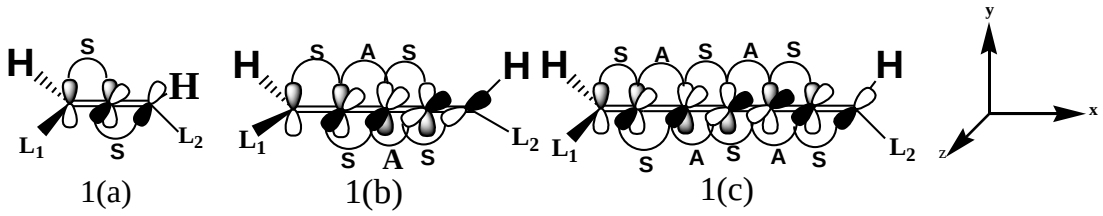

Figure 4.11 Structure of allene based diradical and cumulenes based diradical with phases of HOMO–2. S indicates symmetric and A indicates antisymmetric in the phase of MO. L_1 and L_2 are the left and right radical centers respectively.

For our designed diradicals $HOMO_\alpha$ and $(HOMO–1)_\alpha$ are the nonbonding molecular orbitals, therefore the energy of LUMO decreases and HOMO–2 energy increases remarkably (shown in Figure 4.12) that satisfy the proposal of Imamura et al.[47-49] As a result there is a decrease in the $HOMO_\alpha$–$LUMO_\alpha$ and $(HOMO–2)_\alpha$–$(HOMO–1)_\alpha$ energy gaps.

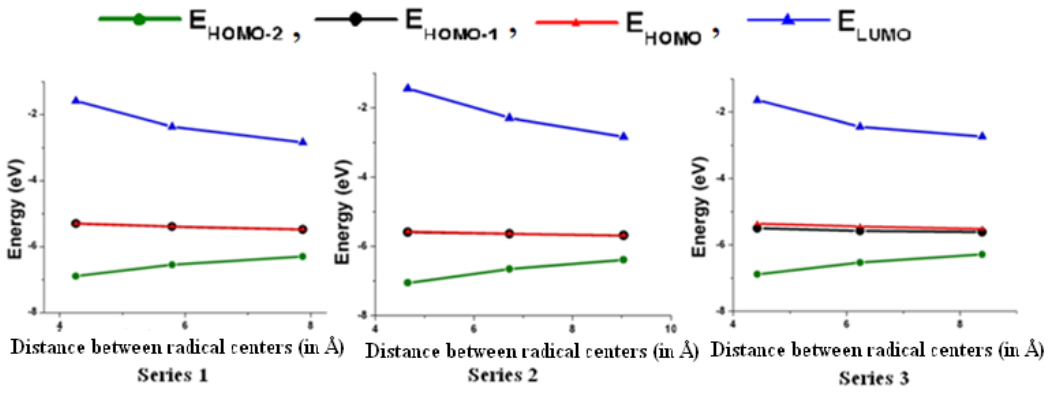

Figure 4.12 Plot of energy vs. distance between radical centers (in Å) for the series 1-3 in their triplet state (B3LYP/6-311++g(d,p)).

To determine the role of LUMO in the magnetic exchange coupling constant, we have computed the electron occupation in LUMO and HOMO–2 and SOMOs (Table 4.7).

Table 4.7 Natural orbital occupation of the diradicals in the triplet state (B3LYP/6-311++G(d,p)).

Systems	HOMO–2	HOMO–1	HOMO	LUMO
1(a)	1.968	1.0	1.0	0.032
1(b)	1.952	1.0	1.0	0.048
1(c)	1.924	1.0	1.0	0.073
2(a)	1.990	1.0	1.0	0.009
2(b)	1.986	1.0	1.0	0.014
2(c)	1.980	1.0	1.0	0.020
3(a)	1.969	1.0	1.0	0.031
3(b)	1.954	1.0	1.0	0.046
3(c)	1.931	1.0	1.0	0.069

From Table 4.7 we can see that LUMOs have considerable amount of occupation. Therefore, it can be assumed that the LUMO takes part in the exchange mechanism. Here, we can see that in case of diradicals (c) in all the series 1-3, the LUMO has the

highest occupation in their respective series. The higher occupation in the LUMO favors strong intramolecular magnetic exchange coupling between the radical centers. Therefore, there is a correlation between the LUMO occupation and magnetic exchange coupling constant.

4.5 Conclusion

All the designed diradicals have ferromagnetic interaction that increases on addition of chiral centers within the coupler. Spin density distribution analysis shows that with the increase in the length of the coupler, enhancement of spin polarization along the coupler takes place and the probability to localize the spin density on each chiral center increases. Addition of chiral centers within the coupler lowers the energy of LUMO and a lower HOMO-LUMO gap facilitates a stronger magnetic coupling and a higher magnetic exchange coupling constant (*J*) results. From natural orbital occupancies it is found that with increasing chain length of chiral coupler the occupancy of LUMO increases. Furthermore, non-applicability of Borden's rule indicates that a good way of predicting the ground state of the diradical systems having allene and [n]-cumulene coupler should be by Hund's rule based spin density alternation. A close inspection of *J* values shows that NN stands for a better choice of radical center over VER and mixed radicals. Thereby, it is expected that this trend might inspire synthetic chemists to synthesis NN- based chiral magnetic molecule with high ferromagnetic interaction. The diradicals with an [n]-cumulene coupler with n being an even number will show antiferromagnetic behavior according to the spin alternation rule. These antiferromagnetic diradicals will be discussed elsewhere.

4.6 References

(1) Nguyen, L. A.; He, H.; Pham-Huy, C. *Int. J. Biomed. Sci*. **2006**, ***2***, 85–100.
(2) Stephens, P. J.; Devlin, F. J.; Pan, J.-J. *Chirality.* **2008**, *20*, 643–663.
(3) Galán-Mascarós, J. R.; Coronado, E.; Goddard, P. A.; Singleton, J.; Coldea, A. I.; Wallis, J. D.; Coles, S. J.; Alberola, A. *J. Am. Chem. Soc*. **2010**, *132*, 9271.
(4) Pappas, C. *Physics* **2012**, *5*, 28.
(5) Train, C.; Gheorghe, R.; Krstic, V.; Chamoreau, L.-M.; Ovanesyan, N.S.; Rikken, G.L.J.A.; Gruselle, M.; Verdaguer, M. *nat. mater.* **2008**, *7*, 729-734.
(6) Togawa, Y.; Koyama, T.; Takayanagi, K.; Mori, S.; Kousaka, Y.; Akimitsu, J.; Nishihara, S.; Inoue, K.; Ovchinnikov, A. S.; Kishine, J. *Phys. Rev. Lett*. **2012**, *108*, 107202.
(7) Wagnière, G. H. *Chem Phys.***1999**, *245*,165–173.

(8) Bordács, S.; Kézsmárki, I.; Szaller, D.; Demko, L.; Kida, N.; Murakawa, H.; Onose, Y.; Shimano, R.; Rõõm, T.; Nagel, U.; Miyahara, S.; Furukawa, N.; Tokura, Y. *Nat. Phys*. **2012**, *8*, 734.
(9) Minguet, M.; Luneau, D.; Paulsen, C.; Lhotel, E.; Gorski, A.; Waluk, J.; Amabilino, D.B.; Veciana, J.; *Polyhedron* **2003**, *22*, 2349-2354.
(10) (a) Ishikawa, I.; Tajima, K. *Solid State Commun.* **1976**, *19*, 525-528.
(b) Yu, X. Z.; Onose, Y.; Kanazawa, N.; Park, J.H.; Han, J.H.; Matsui, Y.; Nagaosa, N.; Tokura, Y. *Nature* **2010,** *465*, 901-904.
(11) Kahn, O. Molecular Magnetism, VCH, New York, 1993.
(12) Coronado E, Delhae` P, Gatteschi D, Molecular magnetism: from molecular assemblies to devices; Miller J. S. (Eds); NATO ASI Series E321, vol 321, Kluwer, Dordrecht, 1996.
(13) Benelli, C.;Gatteschi, D. *Chem.Rev.* **2002**, *102*, 2369-2387.
(14) Lahti, P. M. Magnetic Properties of Organic Materials, Marcel Dekker, New York, 1999.
(15) (a) Kobayashi , H.; Kobayashi , A.; Cassoux, P.; *Chem. Soc. Rev*.**2000**, *29*, 325–333. (b) Uji, S.; Shinagawa, H.; Terashima, T.; Yakabe, T.; Terai , Y.; Tokumoto, M.; Kobayashi, A.; Tanaka, H.; Kobayashi, H. *Nature*.**2001**, *410*, 908–910.
(16) (a) Prinz ,G. A. *Science*, **1998**, *282*, 1660–1663. (b) Emberly, E. G.; Kirczenow, G. *Chem. Phys*. **2002**, *281*, 311–324.
(17) (a) Matsuda, K.; Matsuo, M.; Irie, M. *J. Org. Chem*.**2001**, *66*, 8799–8803. (b) Tanifuji, N.; Irie, M.; Matsuda, K. *J. Am. Chem. Soc*.**2005**, *127*, 13344–13353.
(18) (a) Bhattacharya, D.; Misra, A. *J. Phys. Chem. A*, **2009**, *113*, 5470–5475. (b) Bhattacharya, D.**;** Shil, S.; Misra, A.; Klein, D. J. *Theor. Chem. Acc*., **2010**, *127*, 57–67. (c) Bhattacharya, D.; Shil, S.; Panda, A.; Misra, A. *J. Phys. Chem. A*, **2010**, *114*, 11833–11841.
(19) Ali, Md. E.; Dutta, S.N. *J. Phys. Chem. A* **2006**, *110*, 2776-2784.
(20) (a) Tobe, Y.; Wakabayashi, T.; in *Acetylene Chemistry: Chemistry, Biology, and Material Science* (Eds.: F. Diederich, P. J. Stang, R. R. Tykwinski), Wiley-VCH, Weinheim,**2005**, pp. 387 – 426. (b) Chalifoux, W. A.; Tykwinski, R. R. *Chem. Rec*.**2006**, *6*, 169 –182. c) Shi Shun, A. L. K.; Tykwinski, R. R. *Angew. Chem. Int. Ed*.**2006,** *45*, 1034 – 1057. (d) Raton, B. Polyynes: Synthesis, Properties, and Applications; Cataldo, F. (Eds); Taylor & Francis, **2005**.
(21) Taylor, D. R. *Chem. Rev*.**1967**, *67*, 317.
(22) Hendon, C.H.; Tiana, D.; Murray, A.T.; Carbery, D.R.; Walsh, A. *Chem. Sci*., **2013**, *4*, 4278–4284.
(23) Skibar, W.; Kopacka, H.; Wurst, K.; Salzmann, C.; Ongania, K.H.; Biani, F.F.D.; Zanello.P.; Bildstein, B. *Organometallics* **2004**,*23*,1024-1041.
(24) (a)Januszewski, J.A.; Tykwinski, R.R.; *Chem. Soc. Rev.* **2014**, *43*, 3184-3203.
(b) Januszewski, J.A.; Wendinger, D.; Methfessel, C.D.; Hampel, F.; Tykwinski, R.R.; *Angew. Chem. Int. Ed.***2013**, *52*, 1817 –1821.
(25) Gu, X.; Kaiser, R.I.; Mebel, A.M. *Chem. Phys. Chem.* **2008**, *9*, 350–369.
(26) Prasongkit, J.; Grigoriev, A.; Wendin. G.; Ahuja, R. *Phys. Rev. B* **2010**, *81*, 115404.

(27) Noodleman, L. *J. Chem. Phys.***1981**, *74*, 5737−5743.
(28) Noodleman, L.; Baerends, E. J. *J. Am. Chem. Soc.***1984**, *106*, 2316−2327.
(29) Noodleman, L.; Davidson, E. R. *Chem. Phys.***1986**, *109*, 131−143.
(30) Noodleman, L.; Peng, C. Y.; Case, D. A.; Mouesca, J. -M. *Coord. Chem. Rev.***1995**, *144*, 199−244.
(31) Yamaguchi, K.; Fukui, H.; Fueno, T. *Chem.Lett.***1986**, *15*, 625−628.
(32) Yamaguchi, K.; Takahara, Y.; Fueno, T.; Nasu, K. *Jpn. J. Appl. Phys.***1987**, *26*, L1362−L1364.
(33) Yamaguchi, K.; Jensen, F.;Dorigo, A.; Houk, K. N. *Chem.Phys. Lett.* **1988**, *149*, 537−542.
(34) Yamaguchi, K.; Takahara, Y.; Fueno, T.; Houk, K. N. *Theor. Chim. Acta* **1988**, *73*, 337−364.
(35) Frisch, M. J.; Trucks, G. W.; Schlegel, H. B.; Scuseria, G. E.; Robb, M. A.; Cheeseman, J. R.; Scalmani, G.; Barone, V.; Mennucci, B.; Petersson, G. A.; Nakatsuji, H.; Caricato, M.; Li, X.; Hratchian, H. P.; Izmaylov, A. F.; Bloino, J.; Zheng, G.; Sonnenberg, J. L.; Hada, M.; Ehara, M.; Toyota, K.; Fukuda, R.; Hasegawa, J.; Ishida, M.; Nakajima, T.; Honda, Y.; Kitao, O.; Nakai, H.; Vreven, T.; Montgomery, J. A., Jr.; Peralta, J. E.; Ogliaro, F.; Bearpark, M.; Heyd, J. J.; Brothers, E.; Kudin, K. N.; Staroverov, V. N.; Kobayashi, R.; Normand, J.; Raghavachari, K.; Rendell, A.; Burant, J. C.; Iyengar, S. S.; Tomasi, J.; Cossi, M.; Rega, N.; Millam, M. J.; Klene, M.; Knox, J. E.; Cross, J. B.; Bakken, V.; Adamo, C.; Jaramillo, J.; Gomperts, R.; Stratmann, R. E.; Yazyev, O.; Austin, A. J.; Cammi, R.; Pomelli, C.; Ochterski, J. W.; Martin, R. L.; Morokuma, K.; Zakrzewski, V. G.; Voth, G. A.; Salvador, P.; Dannenberg, J. J.; Dapprich, S.; Daniels, A. D.; Farkas, Ö.; Foresman, J. B.; Ortiz, J. V.; Cioslowski, J.; Fox, D. J. Gaussian, Inc., Wallingford CT, **2009**.
(36) Trindle, C.; Datta, S. N. *Int. J. Quantum Chem.***1996**, *57*, 781-799.
(37) Trindle, C.; Datta, S. N.; Mallik, B. *J. Am. Chem. Soc.***1997**, *119*, 12947-12951.
(38) Hermann, C.; Neugebauer, J.; Gladysz, J. A.; Reiher, M. *Inorg. Chem.* **2005**, *44*, 6174-6182.
(39) Shil, S.; Herrmann, C. *Inorg. Chem.* 2015, *54*, 11733–11740.
(40) Browne, W. R.; Hage, R.; Vos, J. G. *Coord.Chem. Rev.***2006**, *250*, 1653–1668.
(41) Borden, W.T.; Davidson, E.R. *J. Am. Chem. Soc.* **1977**, *99*, 4587–4594.
(42) Borden, W.T.; Davidson, E.R. *Acc. Chem. Res.* **1981**, *14*, 69–76.
(43) Constantinides, C. P.;Koutentis, P. A.; Schatz, J. *J. Am.Chem. Soc.* **2004**, *126*, 16232–16241.
(44) Zhang,G.; Li,S.; Jiang,Y.*J. Phys. Chem. A.* **2003**, *107*, 5573–5582.
(45) Shil, S.; Roy, M.; Misra, A. *RSC Adv.***2015**, *5*, 105574–105582.
(46) Bhattacharya, D.; Shil, S.; Misra, A.; Bytautas, L.; Klein, D. J. *Phys. chem. Chem. Phys.* **2015**, ***17***, 14223-14237.
(47) Aoki, Y.; Imamura, A. *J. Chem. Phys.***1995**, *103*, 9726.
(48) Imamura, A.; Aoki, Y. *Int. J. of Quantum Chem.* **2006**, *106*, 1924 –1933.
(49) Imamura, A.; Aoki, Y. *Int. J. of Quantum Chem.* **2013**, *113*, 423 –427.